

The Global 21 cm Signal of a Network of Cosmic String Wakes

Oscar F. Hernández^{1,2}★

¹*Department of Physics, McGill University, 3600 rue University, Montréal, QC, H3A 2T8, Canada*

²*Marianopolis College, 4873 Westmount Ave., Westmount, QC H3Y 1X9, Canada*

ABSTRACT

In previous works we discussed the 21 cm signature of a single cosmic string wake. However the 21 cm brightness temperature is influenced by a network of cosmic string wakes, and not one single wake. In this work we consider the signal from a network of wakes laid down during the matter era. We also improve on the previous calculation of a single wake signature. Finally we calculate the enhancement of the global 21 cm brightness temperature due to a network of wakes and discuss its effects of the signal measured in the Wouthuysen-Field absorption trough. We estimated that for string tensions between 10^{-8} to 10^{-7} there would be between a 10% to a factor 2 enhancement in the signal.

Key words: Cosmology – cosmic background radiation – dark ages, reionization, first stars – diffuse radiation – intergalactic medium – cosmology: theory

1 INTRODUCTION

In Brandenberger et al. (2010); Hernández & Brandenberger (2012); Hernández (2014) we discussed the signature of a single cosmic string wake in a 21 cm intensity map. However in models which lead to cosmic strings, a network of strings will inevitably form in a phase transition in the early universe. Here we consider the effect that a network of cosmic string wakes will have on the global 21 cm signal. We are particularly interested in the effect these wakes will have on the Wouthuysen-Field (WF) absorption trough in the global signal.

The Experiment to Detect the Global EoR Signature (EDGES) has reported a detection of a stronger-than-expected absorption feature in the 21 cm spectrum (Bowman et al. 2018). This absorption feature would occur in the following way. Before the first luminous sources produced a large enough number of ultraviolet (UV) photons, the 21 cm spin temperature T_S of the cosmic gas was determined by a competition between Compton scattering and collisions. Compton scattering couples T_S to the CMB radiation temperature T_γ , whereas collisions couple T_S to the much cooler kinetic temperature T_K of the cosmic gas. In the presence of Lyman- α ($Ly\alpha$) UV radiation, hydrogen atoms can change hyperfine state, and hence T_S , through the absorption and re-emission of $Ly\alpha$ photons. This is the Wouthuysen-Field (WF) effect (Wouthuysen 1952; Field 1958). The UV photons produced by the first galaxies couple T_S to T_K leading to a more negative brightness temperature. Galaxies also produce X-rays which heat the cosmic gas, and eventually reionization begins. While it is possible that the intergalactic medium (IGM) can be heated to the radiation temperature by X-rays before the spin temperature couples to it, generically there will be a WF absorption trough right after cosmic dawn (Pritchard & Loeb 2010; Mesinger et al. 2013; Mirocha et al. 2016; Fialkov et al. 2016; Park et al. 2019).

Seven years ago we noted that if a WF absorption trough existed, it would lead to the strongest signal from a cosmic string wake (Hernández

2014). If cosmic strings were to exist, the global 21 cm brightness temperature measured by EDGES would be effected not just by one single wake, but by the network of cosmic string wakes. In this paper we recalculate the global 21 cm brightness temperature signal originating from a single wake as well as a network of wakes laid down during the matter era. We begin by reviewing the current experimental limits on the cosmic string tension, and the methods used to obtain them in section 2. In section 3 we describe a cosmic string wake and the string wake network statistics relevant to our calculation. Next, in section 4 we discuss the 21 cm signal from one of these wakes and discuss how the optically thin approximation breaks down in certain situations. We take into account that the wake is sometimes an optically thick medium when averaging over wake orientations, something that was not done in previous calculations (Brandenberger et al. 2010; Hernández & Brandenberger 2012; Hernández 2014). In section 5 we derive the enhancement global signal resulting from a network of cosmic string wakes laid down during the matter era. We focus our attention on the signal between redshifts $z = 14$ to $z = 30$ which includes the redshift range where the WF absorption trough exists. Finally in section 6 we discuss our results and present our conclusions.

2 A REVIEW OF CURRENT LIMITS ON THE COSMIC STRING TENSION

Cosmic strings are linear topological defects, remnants of a high-energy phase transition in the very early Universe, that can form in a large class of extensions of the Standard Model. Their gravitational effects can be parametrized by their string tension $G\mu$, a dimensionless constant where G is Newton’s gravitational constant, and μ is the energy per unit length of the string. Since μ is proportional to the square of the energy scale of the phase transition, placing upper bounds on the string tension is probing particle physics from the top down in an energy range complementary to that probed by particle accelerators such as the Large

★ Email: oscarh@physics.mcgill.ca

Hadron Collider. This string tension is predicted to be between $10^{-8} < G\mu < 10^{-6}$ for Grand Unified models, whereas cosmic superstrings have $10^{-12} < G\mu < 10^{-6}$ (Copeland et al. 2004; Witten 1985). Cosmological observations place limits on the string tension with the magnitude of the signal proportional to $G\mu$.

The gravitational waves emitted by cosmic string loop decay provide a way to detect cosmic strings. Whereas previous pulsar timing array results (Arzoumanian et al. 2016; Ringeval & Suyama 2017; Arzoumanian et al. 2018) placed upper bounds on the string tension, the most recent NANOGrav 12.5 year data set (Arzoumanian et al. 2020) has found hints of a stochastic gravitational wave background (SGWB) that can be interpreted as coming from cosmic strings. The string tension allowed depends on the cosmic string model. Different Nambu-Goto string models with $10^{-11} \lesssim G\mu \lesssim 10^{-8}$ would explain the SGWB observed by NANOGrav (Blasi et al. 2021; Ellis & Lewicki 2021; Bian et al. 2021; Samanta & Datta 2020). In models of metastable cosmic strings string tensions as large as $G\mu \sim 10^{-7}$ could also explain these results (Buchmuller et al. 2020, 2021). However in Abelian-Higgs cosmic string models the cosmic string loops decay by particle emission versus gravitational waves (Hindmarsh et al. 2018). Hence if the SGWB reported by NANOGrav is due to Abelian-Higgs cosmic strings, a fraction of those loops are Nambu-Goto-like and survive to radiate gravitationally. Hindmarsh et al. (2021) find that this fraction needs to be between 10^{-3} and 0.1.

The best current limits on the cosmic string tension come from the CMB angular power spectrum. The Planck collaboration has placed an upper limit on the string tension for Nambu-Goto strings and Abelian-Higgs strings of $G\mu < 1.3 \times 10^{-7}$ and $G\mu < 3.0 \times 10^{-7}$, respectively, at the 95% CL (Planck Collaboration et al. 2014). Finally, there has been much recent research to develop wavelets and machine learning as more sensitive probes of cosmic strings in the CMB (Hergt et al. 2017; McEwen et al. 2017; Vafaei Sadr et al. 2018a,b; Ciuca & Hernández 2017, 2019, 2020, 2021; Ciuca et al. 2019). If the NANOGrav data were to be the SGWB from strings with $10^{-11} \lesssim G\mu \lesssim 10^{-7}$, the work in Ciuca & Hernández (2020, 2021) has show that there is enough information in noisy CMB maps for strings to be detected by machine learning methods.

3 THE COSMIC STRING WAKE NETWORK

The cosmic string network consists of long strings with length larger than the Hubble diameter plus a distribution of string loops with radii smaller than the Hubble radius. Both analytical arguments (Hindmarsh & Kibble 1995) and numerical simulations (Allen & Shellard 1990; Ringeval et al. 2007) tell us that the network of cosmic strings will take on a scaling solution in which the average quantities describing the network are invariant in time if measured in Hubble length $H^{-1}(z)$. Thus the string distribution will be statistically independent on time scales larger than the Hubble radius and its time evolution can be characterized by a random walk with a time step comparable to the Hubble radius. At each time step there will be N_H long cosmic strings per Hubble volume.

Silk & Vilenkin (1984) pointed out that long strings moving perpendicular to the tangent vector along the string give rise to “wakes” behind the string in the plane spanned by the tangent vector to the string and the velocity vector. The wake arises as a consequence of the geometry of space behind a long straight string - space perpendicular to the string is conical with a deficit angle given by $\alpha = 8\pi G\mu$. From the point of view of an observer travelling with the string it appears that matter streaming by the string obtains a velocity kick of magnitude $\delta v = 4\pi G\mu v_s \gamma_s$ towards the plane behind the string.

Here v_s is the velocity of the string, γ_s is the corresponding relativistic gamma factor. This leads to a wedge-shaped region behind the string with twice the background density.

A cosmic string segment laid down at time t_i will generate a wake whose physical dimensions at that time are

$$c_1 t_i \times t_i v_s \gamma_s \times 4\pi G\mu t_i v_s \gamma_s. \quad (1)$$

The dimensions $c_1 t_i$ and $t_i v_s \gamma_s$ span the two length dimensions of the wake and are independent of the string tension. They are both of the order of the instantaneous Hubble radius. The third dimension is the width of the wake, which is much smaller than the length because it is suppressed by the small parameter $G\mu$.

The constant c_1 in equation 1 is the fraction of the long string along which the transverse velocity is positively correlated. Each long string, spanning a Hubble volume, has approximately $1/c_1$ different segments creating $1/c_1$ different wakes. Thus a scaling solution with N_H long strings per Hubble volume will contribute $N_w = N_H/c_1$ wakes. The value of c_1 can be estimated by calculating $\langle v_s(l) v_s(l') \rangle$ with the simulations and code in Ringeval et al. (2007) and this gives $c_1 \approx 0.1$, (C. Ringeval, private communication).

The three wake dimensions evolve with time. After being laid down, the lengths Hubble expand, $l(z) = l(z_i)(z_i + 1)/(z + 1)$, whereas the wake width will grow by gravitational accretion. To analyze the width’s growth we use the Zel’dovich approximation (Zel’dovich 1970) for either shock heated (Brandenberger et al. 2010) or a diffuse wakes (Hernández & Brandenberger 2012). At a later time, parametrized by redshift z , a diffuse wake initialized in the matter era will have grown to physical dimensions (Hernández 2014):

$$l_1(z) \times l_2(z) \times w(z) = \left(\frac{\frac{2}{3} c_1 \sqrt{\frac{z+1}{z_i+1}}}{H(z)} \times \frac{\frac{2}{3} v_s \gamma_s \sqrt{\frac{z+1}{z_i+1}}}{H(z)} \times \frac{G\mu \frac{16\pi}{5} v_s \gamma_s \sqrt{\frac{z+1}{z_i+1}}}{H(z)} \right) \quad (2)$$

where z_i is the redshift that corresponds to time t_i . Note that as time evolves and we move to smaller redshifts, the wake lengths are shrinking in relation to the Hubble radius as $\sqrt{z+1}$ whereas the width is growing by the same factor. Shock heated wakes will be half as wide.

One of the length dimensions as well as the width depend on the transverse velocity v_s of the long string through the quantity $v_s \gamma_s$. This can also be extracted from simulations used in Ringeval et al. (2007) and these give $\langle \gamma_s v_s \rangle \approx 0.4$ (C. Ringeval, private communication), which we will use here, versus the value of $1/\sqrt{3}$ we used in our previous work (Brandenberger et al. 2010; Hernández & Brandenberger 2012; Hernández 2014).

The number density of wakes on a sphere at a fixed redshift z_e is also proportional to $\sqrt{v_s \gamma_s}$. In Appendix A we calculate this as was done in Hernández et al. (2011) by modelling the string world sheet as circular with $\pi r_w^2 = l_1 \times l_2$. However our result here corrects a few details in the original calculation, such as the erroneous factor of $\cos \theta_s$ in the denominator of equation 3.13 in Hernández et al. (2011). We find that the two dimensional number density of wakes intersecting a sphere of radius $R_e = a(z_e)\chi$ is:

$$n_{2D}(z_i, z_e) = \frac{N_w}{3} \sqrt{\pi c_1 v_s \gamma_s} H(z_i)^2 \left(\frac{z_e + 1}{z_i + 1} \right)^2, \quad (3)$$

where N_w is the number of strings per Hubble volume. This is the two dimensional number density of wakes that were laid down at a redshift of z_i and observed on a fixed redshift sphere at redshift z_e .

The average area that an intersecting wake covers on the redshift

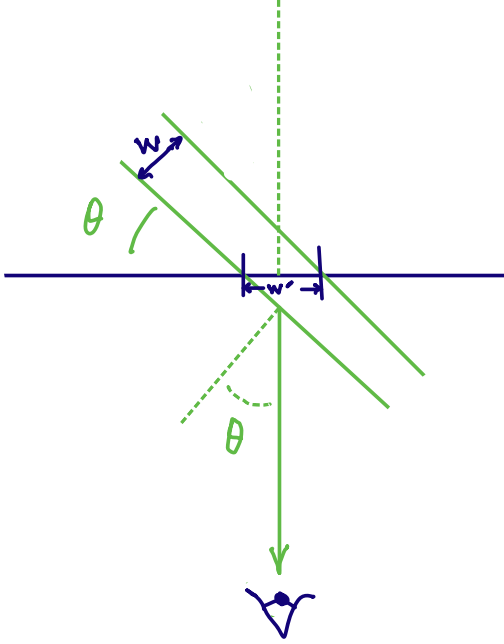


Figure 1. The wake intersection with a very large sphere with the observer at the centre. θ is the angle that the normal to the wake makes with the observer. Note that the effective width intersecting the sphere is $w' = w/\sin \theta$.

sphere is $\langle w' \rangle \times 2r_w$, where w is the wake width and w' is the effective width intersecting the sphere as shown in figure 1. Averaging over all solid angle orientations of the wake disc intersecting this sphere we get:

$$\langle w' \rangle = \int \frac{d\Omega}{4\pi} \frac{w}{\sin \theta} = \frac{1}{4\pi} \int_0^\pi d\theta \sin \theta \int_0^{2\pi} d\phi \frac{w}{\sin \theta} = \frac{\pi}{2} w. \quad (4)$$

Hence the average area that an intersecting wake covers on the redshift sphere is $\pi w r_w$. The fraction of the fixed redshift z_e sphere covered by wakes laid down at redshift z_i is thus

$$\begin{aligned} f(z_i, z_e) &= \pi w r_w n_{2D}(z_i, z_e) \\ &= \left(\frac{32\pi^2}{45} N_w c_1 v_s^2 \gamma_s^2 \right) G\mu \left(\frac{z_e + 1}{z_i + 1} \right)^2 \frac{H_i^2}{H_e^2} \\ &= \left(\frac{32\pi^2}{45} N_w c_1 v_s^2 \gamma_s^2 \right) G\mu \left(\frac{z_i + 1}{z_e + 1} \right) \\ &\approx 11 G\mu \left(\frac{z_i + 1}{z_e + 1} \right) \end{aligned} \quad (5)$$

In the last line we have used the average values discussed above: $N_w c_1 \approx 10$, $\langle v_s \gamma_s \rangle^2 \approx 0.4^2$. We now consider the 21 cm radiation from one single wake on this sphere.

4 THE 21 CM SIGNAL OF A COSMIC STRING WAKE

From Hernández (2014) we have that the optical depth τ_ν for a hydrogen cloud or a cosmic string wake is given by

$$\begin{aligned} \tau_\nu(s) &= \frac{3hc^2 A_{10}}{32\pi v_{21} k_B T_S} [x_{HI} n_H \Delta s \phi(s, \nu)] \\ &\approx [2.583 \times 10^{-12} \text{ mKcm}^2 \text{ s}^{-1}] \frac{1}{T_S} [x_{HI} n_H \Delta s \phi(s, \nu)] \end{aligned} \quad (6)$$

where $A_{10} = 2.85 \times 10^{-15} \text{ s}^{-1}$ is the spontaneous emission coefficient of the 21 cm transition, x_{HI} is the neutral fraction of hydrogen, n_H is the hydrogen number density, Δs is the column thickness of the cosmic hydrogen gas or the string wake, $\phi(s, \nu)$ is the 21 cm line profile, and T_S is the spin temperature.

The distinguishing feature between a cosmic gas and a cosmic string wake is the quantity $[x_{HI} n_H \Delta s \phi(s, \nu)]$. In particular the column length line profile combination for each is

$$[\Delta s \phi(s, \nu)]_{\text{cg}} = \left(\frac{\nu_{21}}{1+z} H(z) \right)^{-1} \quad (7)$$

$$[\Delta s \phi(s, \nu)]_w = [\Delta s \phi(s, \nu)]_{\text{cg}} \sin^{-2}(\theta) \quad (8)$$

for the cosmic gas (cg) and the wake (w), respectively. Here θ is the angle of the 21 cm ray with respect to the vertical to the wake. The optical depth in the cosmic gas is thus,

$$\begin{aligned} \tau_\nu^{\text{cg}}(z) &= \frac{[9.075 \times 10^{-3} \text{ K}]}{T_S} (z+1)^{3/2} \\ &\quad \left(\frac{\Omega_b}{0.05} \sqrt{\frac{0.3}{\Omega_m}} \frac{h}{0.7} \right) \frac{x_{HI} (1 + \delta_b)}{\left(1 + \frac{\partial v_{\text{pec}}/\partial r}{H(z)/(z+1)} \right)}, \end{aligned} \quad (9)$$

where T_S is measured in Kelvin.

For small string tensions ($G\mu < 10^{-7}$) wakes will generically form with no shock heating (Brandenberger et al. 2010; Hernández & Brandenberger 2012). Hence the wake temperature is not significantly different from that of the IGM and the wake baryon density is twice that of the cosmic gas. Hence the optical depth for the wake is:

$$\tau_\nu^w(z) \approx \frac{2 \tau_\nu^{\text{cg}}(z)}{\sin^2(\theta)} \quad (10)$$

The brightness temperature difference, $\delta T_b(\nu)$ is a comparison of the temperature coming from the hydrogen cloud with the ‘‘clear view’’ of the 21 cm radiation from the CMB (Furlanetto et al. 2006).

$$\delta T_b(\nu) = \frac{T_\gamma(\tau_\nu) - T_\gamma(0)}{1+z} = \frac{T_S - T_\gamma(0)}{1+z} (1 - \exp(-\tau_\nu)) \quad (11)$$

We usually have an optically thin medium $\tau_\nu \ll 1$, and hence approximate $(1 - \exp(-\tau_\nu))$ by τ_ν . This approximation holds for the cosmic gas and we will now use it to calculate its brightness temperature. As we will discuss below it does not hold for the brightness temperature of the wake. This point in particular was missed in previous work.

Observing 21 cm radiation depends crucially on T_S . When T_S is above T_γ we have emission, when it is below T_γ we have absorption. Interaction with CMB photons, spontaneous emission, collisions with hydrogen, electrons, protons, and scattering from UV photons will drive T_S to either $T_\gamma = 2.725 \text{ K} (1+z)$ or to T_K . Since the times scales for these processes is much smaller than the Hubble time, the spin temperature is determined by equilibrium in terms of the collision and UV scattering coupling coefficients, x_c and x_α , as well as the kinetic and colour temperatures. Before reionization is significant, $x_{HI} \approx 1$ and the large optical depth of Ly α photons (given by the Gunn-Peterson optical depth) means that the colour temperature is driven to the kinetic temperature $T_K \approx 0.02 \text{ K} (1+z)^2$, of the IGM. Thus we can write the spin temperature as Furlanetto et al. (2006),

$$\begin{aligned} T_S &= T_\gamma \left(\frac{1 + x_c + x_\alpha}{1 + (x_c + x_\alpha) T_\gamma / T_K} \right) \\ &= 2.725 \text{ K} (z+1) \left(\frac{1 + x_c + x_\alpha}{1 + (x_c + x_\alpha) 136/(z+1)} \right). \end{aligned} \quad (12)$$

If we ignore the peculiar velocities and baryon density fluctuations, and take $\Omega_b = 0.05$, $\Omega_m = 0.3$, $h = 0.7$, the optical depth and brightness temperature for the cosmic gas are

$$\tau_\nu^{c_g}(z) = 3.3303 \times 10^{-3} (z+1)^{1/2} \left(\frac{1 + (x_c + x_\alpha) 136 / (z+1)}{1 + x_c + x_\alpha} \right) \quad (13)$$

$$\delta T_b^{c_g}(z) \approx [9.075 \text{ mK}] (1+z)^{1/2} \left[\frac{x_c + x_\alpha}{1 + x_c + x_\alpha} \right] \left(1 - \frac{136}{1+z} \right). \quad (14)$$

We now consider the brightness temperature in the wake. The \sin^{-2} factor present in cosmic string wakes means that when θ is near zero the wake optical depth is large. In previous work (Brandenberger et al. 2010; Hernández & Brandenberger 2012; Hernández 2014) we erroneously approximated this factor by using $\langle \sin^2(\theta) \rangle = 1/2$ and the optically thin approximation. However $\langle \sin^{-2}(\theta) \rangle$ diverges and we need to consider the full $(1 - \exp(-\tau_\nu))$ factor for the brightness temperature of wakes. We note that the average is taken over all solid angles $d\Omega = d(\cos\theta)d\phi$ and not just $d\theta$. Thus we have that the average brightness temperature from a wake is

$$\begin{aligned} \delta T_b^w(z) &\approx \frac{T_S - T_\gamma(0)}{1+z} \langle 1 - \exp(-\tau_\nu^w) \rangle \\ &= \frac{T_S - T_\gamma(0)}{1+z} \int \frac{d\Omega}{4\pi} \left(1 - \exp\left(-\frac{2\tau_\nu^{c_g}}{\sin^2(\theta)}\right) \right) \\ &= \frac{T_S - T_\gamma(0)}{1+z} \int_0^{\pi/2} d\theta \sin\theta \left(1 - \exp\left(-\frac{2\tau_\nu^{c_g}}{\sin^2(\theta)}\right) \right) \end{aligned} \quad (15)$$

The $d\theta$ integral can be evaluated in terms of a Meijer G-function which we Taylor expand since the optical depth of the cosmic gas is small ($\tau_\nu^{c_g} \lesssim 0.1$):

$$\begin{aligned} \int_0^{\pi/2} d\theta \sin\theta \left(1 - \exp\left(-\frac{2\tau}{\sin^2(\theta)}\right) \right) \\ = \tau(-\ln\tau + 1.116) + O(\tau^2 \ln\tau) \end{aligned} \quad (16)$$

and hence the average brightness temperature from a wake is

$$\delta T_b^w(z) \approx \frac{T_S - T_\gamma(0)}{1+z} \tau_\nu^{c_g} (-\ln\tau_\nu^{c_g} + 1.116) \quad (17)$$

and

$$\frac{\delta T_b^w(z)}{\delta T_b^{c_g}(z)} \approx (-\ln\tau_\nu^{c_g} + 1.116) \quad (18)$$

where $\tau_\nu^{c_g}$ is given by equation 13. Using the analysis of the coefficients x_c and x_α from Hernández (2014) we calculate the ratio. For redshifts below 20 the ratio is dominated by the x_α coefficients and for redshifts above 20 it is dominated by the x_c coefficients. We plot the ratio $\delta T_b^w(z)/\delta T_b^{c_g}(z)$ in figure 2. We see that at $z = 17$ its value is about 3.7 and 4.9 for Pop II and Pop III stars, respectively.

Eventually x-rays will heat the cosmic gas raising the spin temperature and destroying the WF absorption trough. Our calculation of the brightness temperature does not take this into account, and hence our calculations should not be applied at redshifts below the WF absorption trough, i.e. $z \lesssim 15$.

5 THE GLOBAL 21 CM SIGNAL OF THE WAKE NETWORK

The fraction $f(z_i, z_e)$ of the fixed redshift z_e sphere covered by wakes that were laid down at redshift z_i is given by equation 5. The

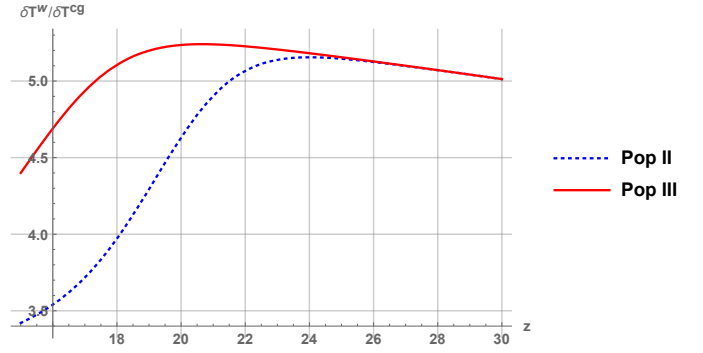


Figure 2. The ratio of the average brightness temperature from a cosmic string wake compared to that of the cosmic gas, for Pop II and Pop III stars.

global 21 cm signal from this network of wakes at a redshift z_e that were laid down at a redshift z_i is $f(z_i, z_e) \times \delta T_b^w(z_e)$. Since $f(z_i, z_e)$ is proportional to the string tension, it is much less than one the fraction of the sphere covered by wakes laid down during the matter era can be approximated by integrating $f(z_i, z_e)$ between z_e and $z_i = z_{\text{eq}} \approx 3400$. For this result to be accurate to within say 15%, we would need to check that this integral is less than $\sqrt{0.15} = 0.39$. We will see below that for the cases of interest to us this is indeed the case.

Given the above, the global brightness temperature coming from z_e is approximately

$$\begin{aligned} \delta T_b^{c_g}(z_e) \left(1 - \int_{z_{\text{eq}}}^{z_e} dz_i f(z_i, z_e) \right) + \delta T_b^w(z_e) \left(\int_{z_{\text{eq}}}^{z_e} dz_i f(z_i, z_e) \right) \\ \delta T_b^{c_g}(z_e) + \int_{z_{\text{eq}}}^{z_e} dz_i f(z_i, z_e) (\delta T_b^w(z_e) - \delta T_b^{c_g}(z_e)) \\ = \delta T_b^{c_g}(z_e) \left[1 + \left(\frac{\delta T_b^w(z_e)}{\delta T_b^{c_g}(z_e)} - 1 \right) \int_{z_e}^{z_{\text{eq}}} dz_i f(z_i, z_e) \right] \end{aligned} \quad (19)$$

The quantity in brackets is the factor by which the brightness temperature is enhanced because of the cosmic string wake network. We will call this factor F .

$$F \equiv \left[1 + \left(\frac{\delta T_b^w(z_e)}{\delta T_b^{c_g}(z_e)} - 1 \right) \int_{z_e}^{z_{\text{eq}}} dz_i f(z_i, z_e) \right] \quad (20)$$

Using equation 5 we can evaluate the integral in the second term of F with $z_{\text{eq}} = 3400$:

$$\int_{z_e}^{z_{\text{eq}}} dz_i f(z_i, z_e) = 5.5 G\mu \frac{(z_{\text{eq}} + 1)^2}{(z_e + 1)} = \frac{6.5 \times 10^7}{(z_e + 1)} G\mu. \quad (21)$$

For $z_e > 17$ and $G\mu < 10^{-7}$, this integral is less than 0.37.

Thus for wakes laid down during the matter dominated period, we have

$$F \approx 1 + \left(\frac{\delta T_b^w(z_e)}{\delta T_b^{c_g}(z_e)} - 1 \right) \frac{6.5 \times 10^7}{(z_e + 1)} G\mu \quad (22)$$

In figure 3 we plot $(F - 1)/(G\mu)$. At $z_e = 17$, which is where the EDGES absorption profile is centred, $F \approx 1 + 0.98 \times 10^7 G\mu$ and $F \approx 1 + 1.4 \times 10^7 G\mu$, for Pop II and Pop III stars, respectively. Thus a string tension between 10^{-8} to 10^{-7} would lead to a 10% to a factor 2 enhancement in the signal.

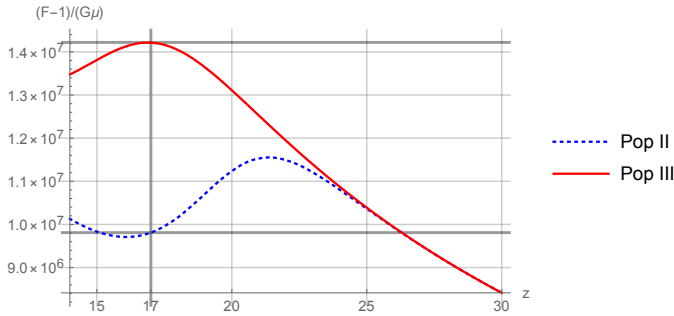


Figure 3. The enhancement factor $(F - 1)/(G\mu)$ for Pop II and Pop III stars.

6 DISCUSSION AND CONCLUSIONS

The work in [Hernández \(2014\)](#) calculated the global 21 cm signal of a single cosmic string wake and made the case that such a place is the best place to look for them. In the present work we have improved on the analysis by improving the calculation of the signal of one wake and considering the effect that a network of wakes laid down during the matter era would have on the signal. We estimated that for string tensions between 10^{-8} to 10^{-7} there would be between a 10% to a factor 2 enhancement in the signal.

The most recent NANOGrav results on the stochastic gravitational wave background admit a cosmic string interpretation with string tensions between 10^{-11} to 10^{-7} . The encouraging results of this first analysis justifies a more thorough and rigorous work which would consider the contribution of wakes initialized during the radiation era and numerical calculations of quantities we have estimated (work in progress with C. Ringeval).

ACKNOWLEDGEMENTS

I am very grateful to Christophe Ringeval for many fruitful discussions and comments on this work. This work was made possible by the support of the Fonds de recherche du Québec – Nature et technologies (FRQNT) Programme de recherche pour les enseignants de collège, (funding reference number 2021-CO-283996).

DATA AVAILABILITY

The data underlying this article will be shared on reasonable request to the corresponding author.

REFERENCES

Allen B., Shellard E. P. S., 1990, *Phys. Rev. Lett.*, 64, 119
 Arzoumanian Z., et al., 2016, *ApJ*, 821, 13
 Arzoumanian Z., et al., 2018, *ApJ*, 859, 47
 Arzoumanian Z., et al., 2020, *ApJL*, 905, L34
 Bian L., Cai R.-G., Liu J., Yang X.-Y., Zhou R., 2021, *Phys. Rev. D*, 103, L081301
 Blasi S., Brdar V., Schmitz K., 2021, *Phys. Rev. Lett.*, 126, 041305
 Bowman J. D., Rogers A. E. E., Monsalve R. A., Mozdzen T. J., Mahesh N., 2018, *Nature*, 555, 67
 Brandenberger R. H., Danos R. J., Hernández O. F., Holder G. P., 2010, *J. Cosmol. Astropart. Phys.*, 2010, 028
 Buchmuller W., Domcke V., Schmitz K., 2020, *Phys. Lett. B*, 811, 135914
 Buchmuller W., Domcke V., Schmitz K., 2021, ArXiv e-print, 2107.04578
 Ciuca R., Hernández O. F., 2017, *J. Cosmol. Astropart. Phys.*, 2017, 028

Ciuca R., Hernández O. F., 2019, *MNRAS*, 483, 5179
 Ciuca R., Hernández O. F., 2020, *MNRAS*, 492, 1329
 Ciuca R., Hernández O. F., 2021, *MNRAS*, 506, 1406
 Ciuca R., Hernández O. F., Wolman M., 2019, *MNRAS*, 485, 1377
 Copeland E. J., Myers R. C., Polchinski J., 2004, *J. High Energy Phys.*, 2004, 013
 Ellis J., Lewicki M., 2021, *Phys. Rev. Lett.*, 126, 041304
 Fialkov A., Cohen A., Barkana R., Silk J., 2016, *MNRAS*, 464, 3498
 Field G. B., 1958, Proceedings of the IRE, 46, 240
 Furlanetto S. R., Oh S. P., Briggs F. H., 2006, *Physics Reports*, 433, 181
 Hergt L., Amara A., Brandenberger R. H., Kacprzak T., Refregier A., 2017, *J. Cosmol. Astropart. Phys.*, 2017, 004
 Hernández O. F., 2014, *Phys. Rev. D*, 90, 123504
 Hernández O. F., Brandenberger R. H., 2012, *J. Cosmol. Astropart. Phys.*, 2012, 032
 Hernández O. F., Wang Y., Fong J., Brandenberger R. H., 2011, *J. Cosmol. Astropart. Phys.*, 2011, 014
 Hindmarsh M., Kibble T. W. B., 1995, *Reports on Progress in Physics*, 58, 477
 Hindmarsh M., Lizarraga J., Urrestilla J., Daverio D., Kunz M., 2018, *Phys. Rev. D*, 99, 449
 Hindmarsh M., Lizarraga J., Urrio A., Urrestilla J., 2021, ArXiv e-print, 2103.16248
 McEwen J. D., Feeney S. M., Peiris H. V., Wiaux Y., Ringeval C., Bouchet F. R., 2017, *MNRAS*, 472, 4081
 Mesinger A., Ferrara A., Spiegel D. S., 2013, *MNRAS*, 431, 621
 Mirocha J., Furlanetto S. R., Sun G., 2016, *MNRAS*, 464, 1365
 Park J., Mesinger A., Greig B., Gillet N., 2019, *MNRAS*, 484, 933
 Planck Collaboration et al., 2014, *A&A*, 571, A25
 Pritchard J. R., Loeb A., 2010, *Phys. Rev. D*, 82, 023006
 Ringeval C., Suyama T., 2017, *J. Cosmol. Astropart. Phys.*, 2017, 027
 Ringeval C., Sakellariadou M., Bouchet F. R., 2007, *J. Cosmol. Astropart. Phys.*, 2007, 023
 Samanta R., Datta S., 2020, arXiv, 2009.13452v3
 Silk J., Vilenkin A., 1984, *Phys. Rev. Lett.*, 53, 1700
 Vafaie Sadr A., Movahed S. M. S., Farhang M., Ringeval C., Bouchet F. R., Bouchet F. R., 2018a, *MNRAS*, 475, 1010
 Vafaie Sadr A., Farhang M., Movahed S. M. S., Bassett B., Kunz M., 2018b, *MNRAS*, 478, 1132
 Witten E., 1985, *Phys. Lett. B*, 153, 243
 Wouthuysen S. A., 1952, *AJ*, 57, 31
 Zel'dovich Y. B., 1970, *A&A*, 5, 84

APPENDIX A: THE WAKE NUMBER DENSITY

The two dimensional number density n_{2D} of wakes intersecting a sphere inside a Hubble volume is given by the product of the expected number of string wakes laid down in a Hubble volume, N_w , and the probability P of a wake intersecting that sphere, divided by the surface area $4\pi R^2$ of the sphere: $n_{2D} = N_w P / (4\pi R^2)$. We calculate this below.

We consider a string wake of physical dimensions $l_1 \times l_2 \times w$ laid down at time t_i . To simplify our analysis we model this wake as an equal volume thin coin-like disc of radius r_w , where $\pi r_w^2 = l_1 l_2$. Consider a physical Hubble volume at this same time t_i that contains this wake and a sphere of physical radius R' . We take the Hubble volume to have the shape of a cylinder with axis parallel to the wake disc axis, as shown in figure A1. The probability P is the volume where the wake disc touches the R' sphere divided by the cylinder's volume. Set up cylindrical coordinates at the origin of this sphere

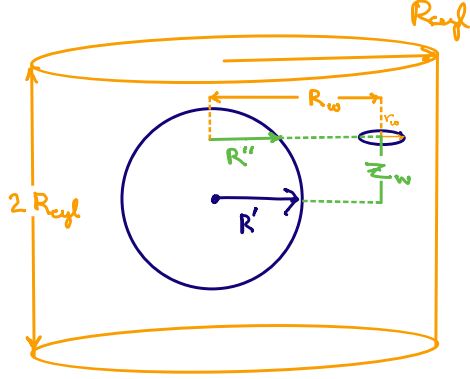


Figure A1. A cylindrically shaped Hubble volume containing a string wake and a sphere.

and let z_w, R_w, ϕ_w be the coordinates of the wake. Then

$$\begin{aligned}
 P &= \frac{1}{V_{\text{cylinder}}} \int_{-R'}^{R'} dz_w \int_0^{R_{\text{cylinder}}} dR_w \int_0^{2\pi} d\phi_w \int_0^{R_{\text{cylinder}}} dR'' \\
 &\quad \left[\Theta((R'' + r_w) - R_w) \Theta(R_w - (R'' - r_w)) \right. \\
 &\quad \quad \left. \delta^D(R'' - (R'^2 - z_w^2)^{1/2}) \right] \\
 &= \frac{2\pi^2 R'^2 r_w}{V_{\text{cylinder}}} \tag{A1}
 \end{aligned}$$

Since $V_{\text{cylinder}} \approx H(t_i)^3$ we have that the expected number of wakes intersecting the sphere at time t_i is

$$\langle N_{S^2} \rangle = N_w P = N_w H_i^3 2\pi^2 R'^2 r_w \tag{A2}$$

We are interested in the two dimensional number density n_{2D} of wakes that were laid down at a redshift of z_i and observed on a fixed redshift sphere at redshift z_e . The sphere from which the observed radiation is emitted has $R_e = a_e \chi_e$, but it had radius $R' = a_i \chi_i$ when the wakes were laid down. And thus dividing equation A2 by $4\pi R_e^2$ we get

$$\begin{aligned}
 n_{2D}(z_i, z_e) &= N_w H_i^3 2\pi^2 r_w \left(\frac{z_e + 1}{z_i + 1} \right)^2 \tag{A3} \\
 &= \frac{N_w}{3} \sqrt{\pi c_1 v_s \gamma_s} H(z_i)^2 \left(\frac{z_e + 1}{z_i + 1} \right)^2
 \end{aligned}$$

where in the last line we have used $r_w = H_i^{-1} 2/3 \sqrt{c_1 v_s \gamma_s / \pi}$ as can be seen from equation 1.

This paper has been typeset from a $\text{\TeX}/\text{\LaTeX}$ file prepared by the author.